Electrocardiogram (ECG) patterns of left anterior fascicular block and conduction impairment in ventricular myocardium: a whole-heart model-based simulation study

Gao, Y., Xia, L., Gong, Y. & Zheng, D.

Author post-print (accepted) deposited by Coventry University's Repository

Original citation & hyperlink:
Gao, Y, Xia, L, Gong, Y & Zheng, D 2018, 'Electrocardiogram (ECG) patterns of left anterior fascicular block and conduction impairment in ventricular myocardium: a whole-heart model-based simulation study' Journal of Zhejiang University: Science B, vol. 19, no. 1, pp. 49–56.
https://dx.doi.org/10.1631/jzus.B1700029

DOI 10.1631/jzus.B1700029
ISSN 1673-1581
ESSN 1862-1783

Publisher: Springer

The final publication is available at Springer via http://dx.doi.org/10.1631/jzus.B1700029

Copyright © and Moral Rights are retained by the author(s) and/ or other copyright owners. A copy can be downloaded for personal non-commercial research or study, without prior permission or charge. This item cannot be reproduced or quoted extensively from without first obtaining permission in writing from the copyright holder(s). The content must not be changed in any way or sold commercially in any format or medium without the formal permission of the copyright holders.

This document is the author's post-print version, incorporating any revisions agreed during the peer-review process. Some differences between the published version and this version may remain and you are advised to consult the published version if you wish to cite from it.

Electrocardiographic patterns of left anterior fascicular block and conduction impairment in ventricular myocardium: A whole-heart model based simulation study

Yuan Gao[1], Ling Xia[1*], Yinglan Gong[1*], Dingchang Zheng[2]

[1] Department of Biomedical Engineering, Zhejiang University, Hangzhou 310027, China

[2] Health and Wellbeing Academy, Faculty of Medical Science, Anglia Ruskin University, Chelmsford, CM1 1SQ, UK

* xialing@zju.edu.cn; yinglangong@zju.edu.cn

Abstract

Left anterior fascicular block (LAFB) is a heart disease identifiable from an abnormal electrocardiogram (ECG). It has been reported that LAFB is associated with an increased risk of heart failure. Non-specific intraventricular conduction delay due to the lesions of the conduction bundles and slow cell to cell conduction has also been considered as another cause of heart failure. Since the location and mechanism of conduction delay have notable variability between individual patients, we hypothesized that the impaired conduction in the ventricular myocardium may lead to abnormal ECGs similar to LAFB ECG patterns. To test this hypothesis, in this study, based on a computer model with three dimensional whole-heart anatomical structure, we simulated the cardiac exciting sequence map and 12-lead ECG caused by the block in the left anterior fascicle and by the slow conduction velocity in the ventricular myocardium. The simulation results showed that the typical LAFB ECG patterns can also be observed from cases with slow conduction velocity in the ventricular myocardium. The main differences were the duration of QRS and wave amplitude. In conclusion, our simulations provide a promising starting point to further investigate underlying mechanism of heart failure with LAFB, which would provide potential reference for LAFB diagnosis.

Keywords: conduction delay, ECG simulation, heart model, Left anterior fascicular block (LAFB)

1 Introduction

Left anterior fascicular block (LAFB) is caused by conduction failure or slowed conduction in the left anterior fascicle. The left anterior fascicle is delicate to injury leading to high incidence rate of LAFB because the left anterior fascicle is thin and long, is crossing the left ventricular out-flow tract, and blood is supplied from a single vessel. LAFB has usually been considered a benign

electrocardiographic finding [1], it is therefore often neglected. Recent studies showed that LAFB in the elderly patients could be a useful clinical marker for various cardiovascular diseases, which is associated with an increased risk of atrial fibrillation, heart failure and even death [2,3]. LAFB has recently attracted increasing attention [4-6].

Many studies with heart failure patients have revealed heterogeneous left ventricular (LV) activation patterns with different locations and extents of specific ventricular delays [7-9]. The conduction delay may be due to the lesions of the conduction bundles and slow cell-to-cell conduction, leading to mechanical dyssynchrony and ventricular systolic dysfunction [10]. Since the locations and mechanisms of conduction delay have significant variability between individual patients, a better understanding of their mechanisms would help disease diagnosis therefore increase the therapy efficacy.

12-lead electrocardiogram (ECG) has been widely accepted as the main noninvasive diagnostic method of cardiac diseases [11]. However, current diagnosis by the 12-lead ECG suffers from some limitations. For instance, it could be insensitive because some cardiac diseases may have similar waveform patterns. Previous studies on the cardiac resynchronization therapy for patients with left bundle branch block (LBBB) have identified that slow conduction in the impaired working myocardium of the left ventricular could lead to the similar ECG patterns of LBBB, and the pathological working myocardium contributes to the intraventricular conduction delay of the LV, which combining with the alterations His system leads to an overall deterioration of cardiac function [12,13]. We therefore hypothesized that the impaired conduction in the ventricular myocardium may also lead to abnormal ECGs similar to LAFB ECG patterns.

This study aimed to simulate and compare the cardiac exciting sequence map and 12-lead ECG of LAFB in two clinical situations: (1) complete LAFB; (2) slow conduction velocity in the anterior LV myocardium.

2 Methods

2.1 Anatomical Model

The heart specimen containing atria and ventricle was obtained from a healthy male adult in Zhujiang Hospital, Southern Medical University, China. The use of the heart for research purpose was approved by the local Ethics Committee of the Southern Medical University. The National Rules and Regulations on Heart research were strictly followed. The specimen was scanned by spiral computer tomography (Philips / Brilliance 64) with a resolution of 512 pixels by 512 pixels and a

spatial resolution of 0.3574×0.3574×0.33 mm (Figure 1 A and B). Details of the model were described in our previous study [14,15].

In the model, the conduction system included sinoatrial node, Bachmann's bundle, crista terminalis, pectinate muscles, atrial-ventricular node, His bundle, left and right bundles and Purkinje fibers. During the propagation, each myocardial unit has specific electrophysiological parameters associated with the action potential of the cell unit and conduction velocity. In order to simulate the anisotropy, the myocardial fiber orientation was contained. The excitation conduction velocity along the fiber was set to be three times larger than that in the transverse direction within the physiological ranges. The atrial cell in our study was based on the model developed by Courtemanche et al [16], and the ventricular cell model from the refined ten Tusscher et al [17].

2.2 Numerical Method

The propagation of action potential was based on the monodomain model [18]:

$$\frac{\partial V_m}{\partial t} = \frac{1}{C_m}\left(\frac{1}{A_m}\left(\frac{\lambda}{1+\lambda}\nabla\cdot\left(\sigma_i\nabla Vm\right) - I_{ion} + I_{app}\right)\right) \quad (1)$$

where V_m is transmembrane voltage, C_m is the membrane capacitance, A_m is surface-to-volume ratio, σ_i is cellular conductivity, I_{ion} is the sum of ionic currents, I_{app} is the sum of applied stimulus currents.

The equation was solved numerically using explicit Euler method based on parallel computational techniques.

The torso model in our study was taken from the virtual male subject of the United States (Figure 1 C). To calculate the body surface potential generated by the cardiac sources, the equation can be expressed as

$$\Phi\left(r_t\right) = \frac{1}{4\pi\sigma}\left(\int_{\Omega_h} J_s\cdot\nabla\left(\frac{1}{\left|r_t - r\right|}\right)dV + \sum_{l=1}^{m}\left(\sigma_l^{+} - \sigma_l^{-}\right)\int_{S_l}\Phi\left(r\right)\nabla\left(\frac{1}{\left|r_t - r\right|}\right)dS\right) \quad (2)$$

where r_t is the field point in the torso volume conductor, σ is the conductivity of this point, Ω_h is the heart area, S_l is the conductivity junction surface, and its inside and outside conductivities are σ_l^- and σ_l^+, respectively.

2.3 Simulations of LAFB and Slow Conduction Velocity

By blocking excitation propagation at the points of the left anterior branch near the anterior papillary muscle, we simulated the cardiac exciting sequence map and 12-lead ECG of LAFB. The conduction delay in the left ventricle anterior wall was simulated by slowing the conduction velocity

of the myocardium to 20%. For comparison, we also show the exciting sequence map and 12-lead ECG in the normal case.

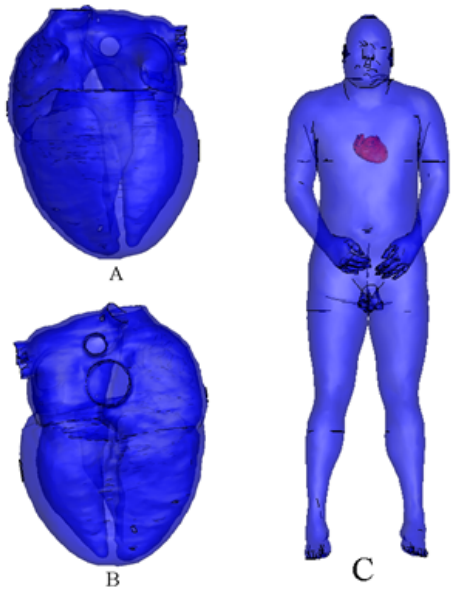

Figure 1. Model of the heart and torso: (A) anterior view of the heart; (B) posterior view of the heart; (C) the merge of the heart into the body.

3 Results

3.1 Normal exciting sequence map and 12-lead ECG

Figure 2 shows four typical cardiac activation sequence maps. The initial onset of LV endocardial activation was located at the septum, then at anterior and posterior wall at 112 msec, the confluent of the three areas at 120 msec, the epicardial excitation at 135 msec and the latest activation at the basal at the time of 196 msec. Our simulation results agreed with the experimental data [19].

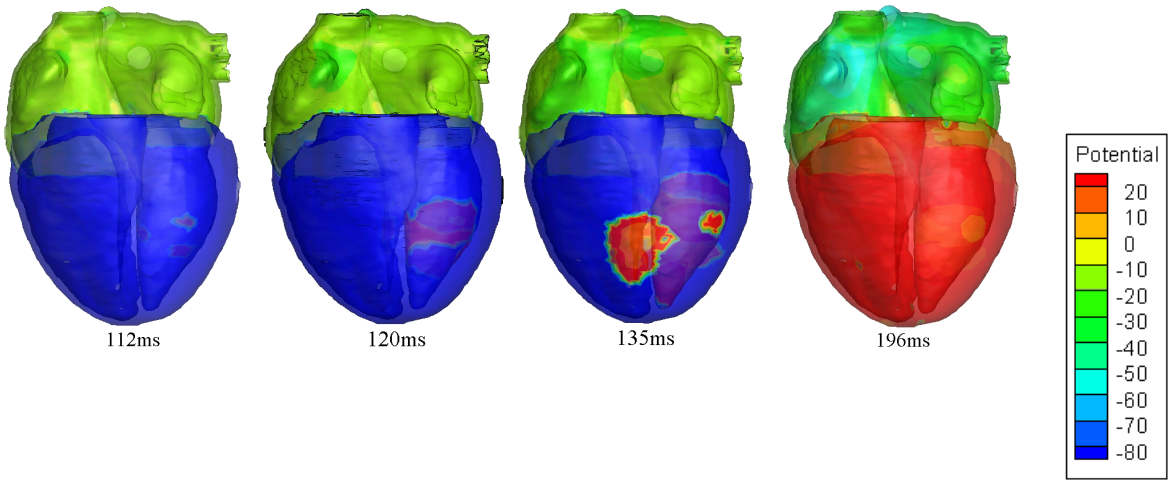

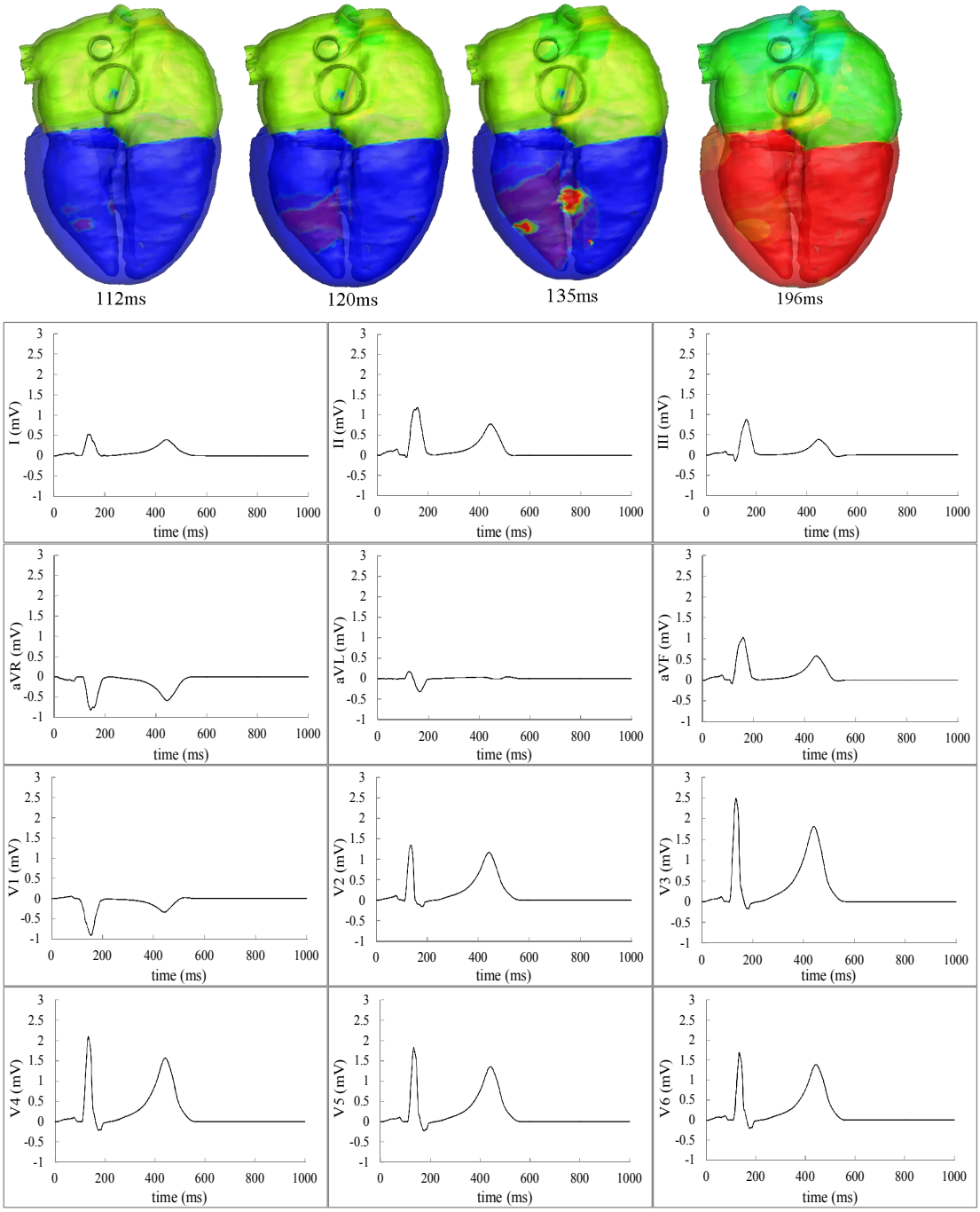

Figure 2. Simulated activation sequences and 12 lead ECG of a normal heart. First row: the anterior view of the heart. Second row: the posterior view of the heart. The translucent surface is the epicardium, the opaque surface represents the endocardium. The numbers indicate the time instants of depolarization in milliseconds. The color bar with potential amplitude is shown on the right-hand side of the maps. Last four rows: 12 lead ECG

3.2 Effect of compete LAFB on cardiac exciting sequence map and 12-lead ECG

Figure 3 shows the simulation results with the complete LAFB. The left anterior branch was blocked, and the initial excitation of the LV free wall was yielded by the left posterior fascicular. The

excitation propagated from endocardium to epicardium, with the orientation to the bottom-right.

In comparison with the simulation from normal heart, LAFB made the propagation point to the top-left missed, resulting in the occurrence of Q wave at lead aVL. Next, since the conduction velocities of the Purkinje fibers and endocardial are very fast, the excitation at the ventricular septum propagated quickly to the LV anterior wall that made the propagation point to the top-left. So lead aVL showed a significant R wave whereas leads II, III, and aVF showed S wave. For leads V3 to V6 the R wave decreased and S wave deepened. The total duration of ventricular repolarization was 205 msec, slightly longer than that of the normal case.

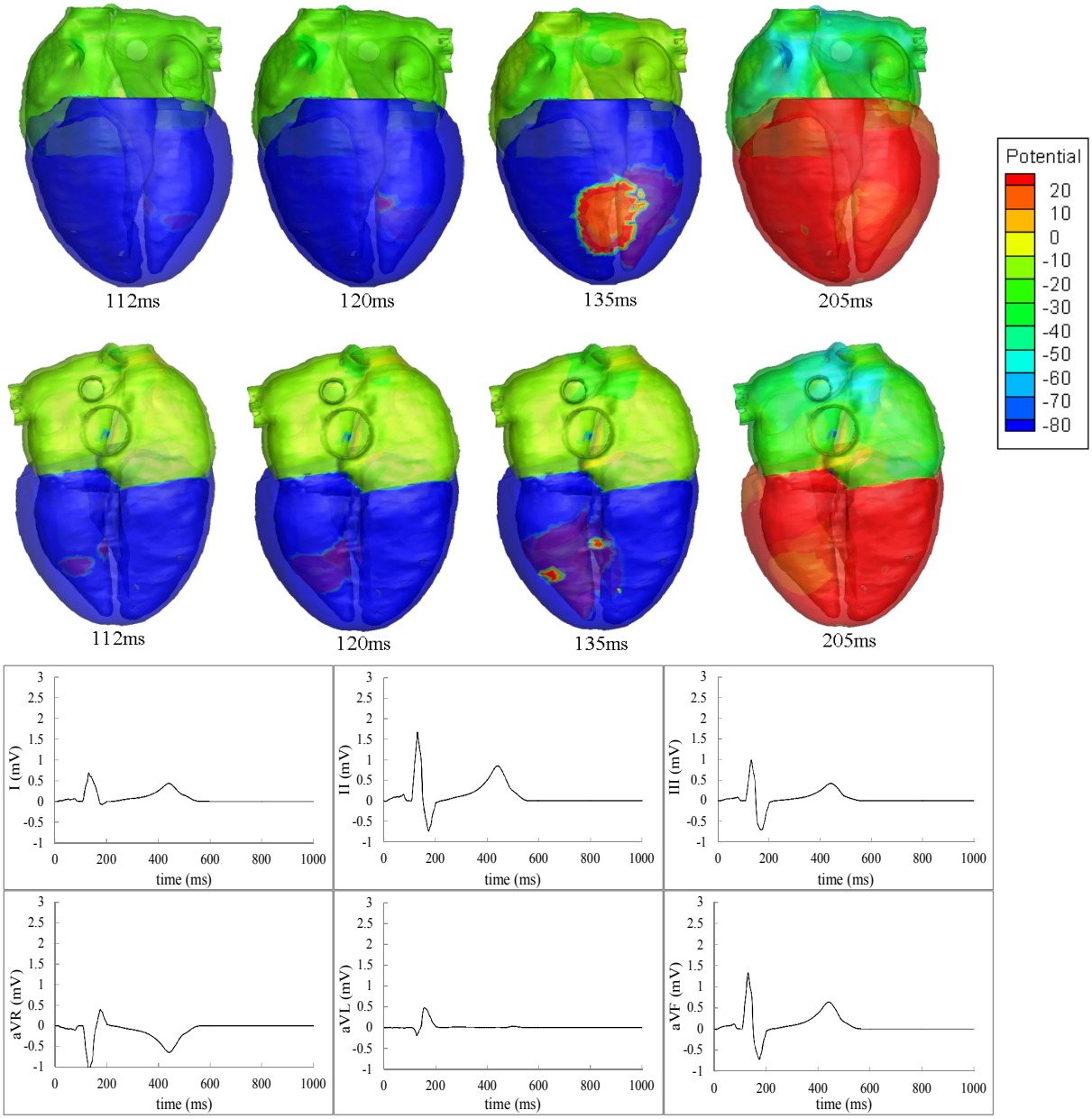

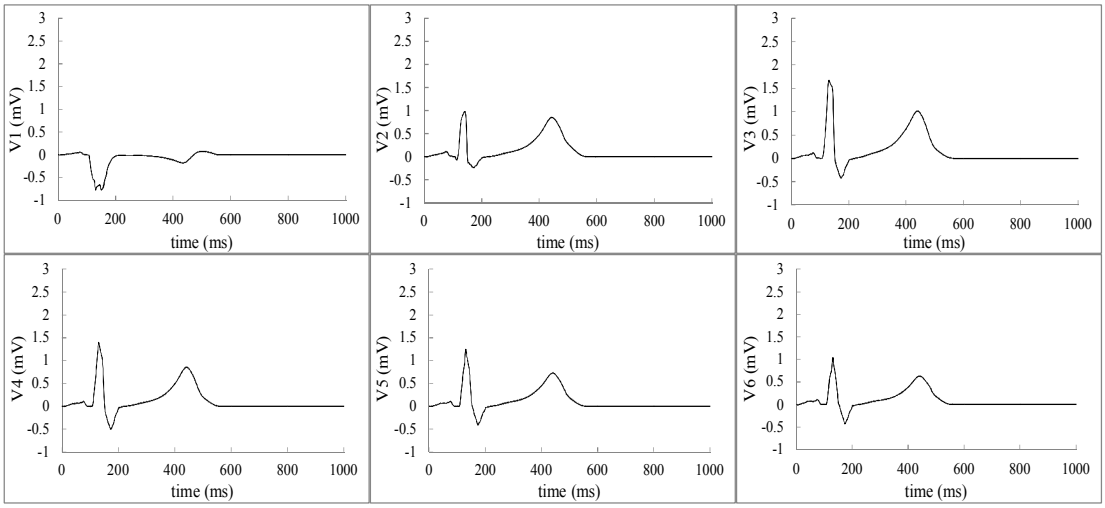

Figure 3. Simulated activation sequences and 12 lead ECG of the complete LAFB. (refer to the description of Figure 2)

3.3 Effect of slow conduction velocity of the ventricular myocardium on cardiac exciting sequence map and 12-lead ECG

As shown in Figure 4, the initial onset of activation was the same as the normal case. However, the excitation moved slowly in the anterior wall while much quickly in the posterior wall, leading to a relatively weak wave pointing to top-left and a relatively strong wave pointing to bottom-right. This resulted lead aVL showed Q wave. Since the conduction in the anterior wall was slow, the depolarization was completed early in the posterior wall, and the last activated area was the anterior wall that made the propagation point to the top-left. So lead aVL showed R wave, leads II, III, and aVF showed S wave. For leads V3 to V6 the R wave decreased and S wave deepened.

The total duration of ventricular repolarization was 225 msec, longer than that of the LAFB.

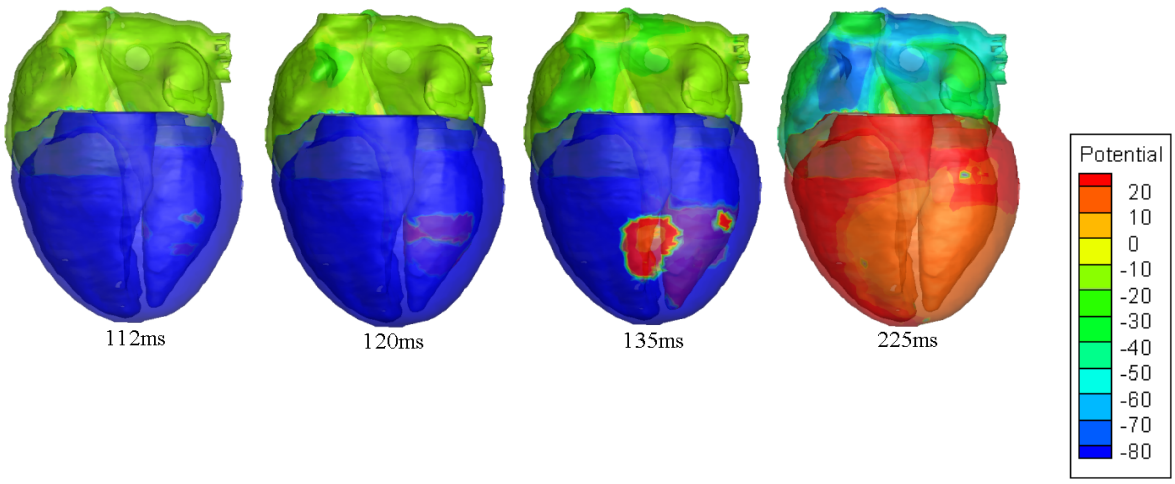

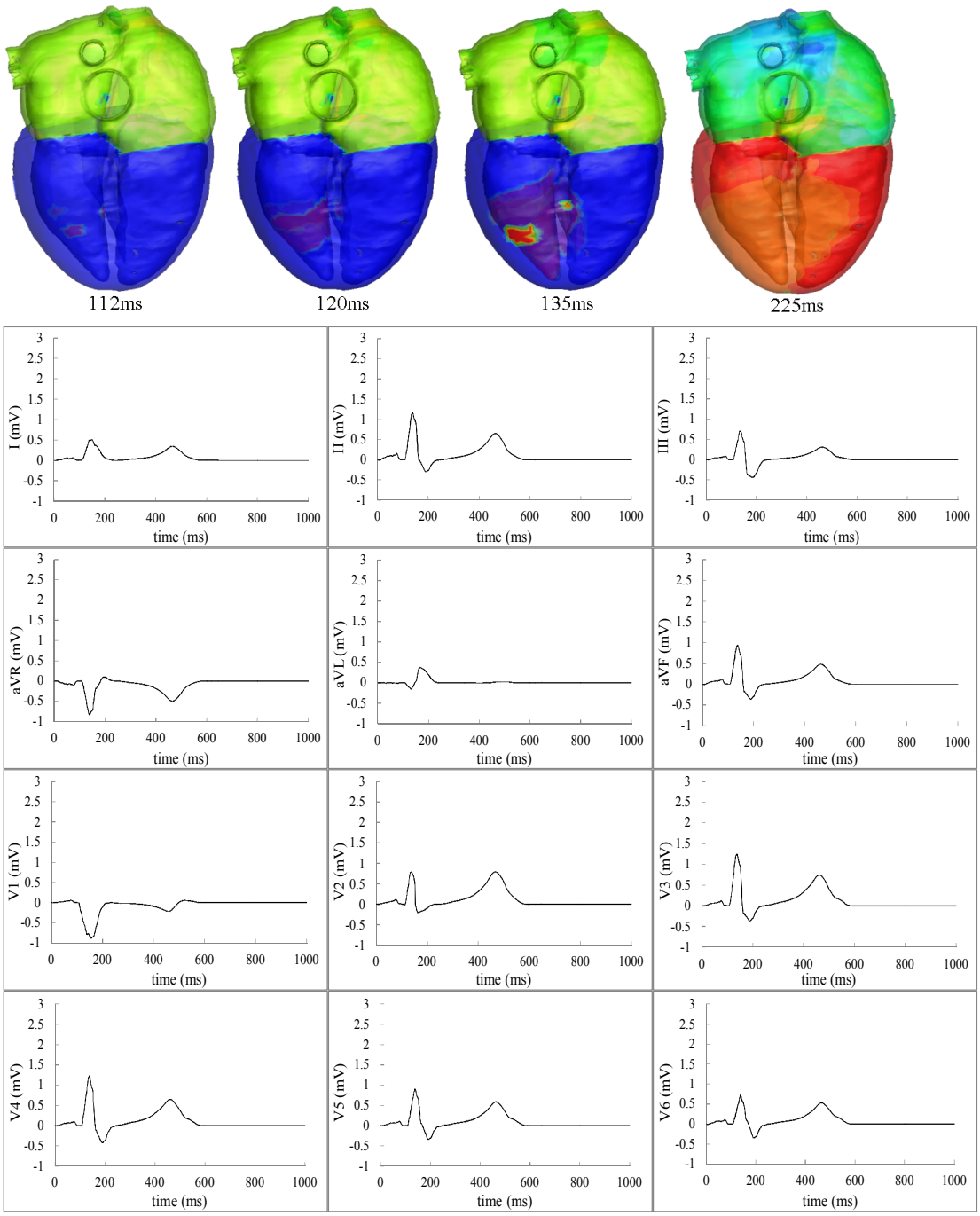

Figure 4. Simulated activation sequences and 12 lead ECG of slow conduction velocity in myocardium. (refer to the description of Figure 2)

3.3 Comparison of the effect of compete LAFB and slow conduction velocity of the ventricular myocardium

It is noted that there were some similar effect of LAFB and slowed conduction velocity on the ECG patterns, but the wave amplitude and QRS duration on each lead were different. On lead aVL, at the beginning of LV activation, the slow conduction in the anterior wall made a relatively minor degree missing of wave propagation pointing to the top-left just like LAFB, and generated a Q wave

with smaller amplitude. Later, when the curve turned to the positive direction, for the same reason, the slow conduction resulted in smaller amplitude of R wave. On leads II, III, and aVF, the last activated area in the anterior wall resulting in the occurrence of S wave, but due to the slow conduction of the propagation, the S wave were broad and gentle (see Figure 4). This reason can also explain the difference on other leads. Table 1 shows the detail comparison of the maximum and minimum amplitude of QRS on each lead of LAFB and slow conduction velocity of the ventricular myocardium. The amplitude of QRS with slow conduction velocity of the ventricular myocardium reduced the range from 16% to 59.5% compared to the LAFB. So the presences of decreased amplitude and prolonged duration of QRS are indicators of impaired conduction in ventricular myocardium.

Table 1. The maximum and minimum amplitude of QRS on each lead of LAFB and slow conduction velocity of the ventricular myocardium. (SCV indicates slow conduction velocity of the ventricular myocardium. The unit of the amplitude is millivolt.)

	aVL		aVF		II		III		V3		V4		V5		V6	
	Max	Min	Max	Min	Max	Min	Max	Min	Max	Min	Max	Min	Max	Min	Max	Min
LAFB	0.48	-0.20	1.33	-0.72	1.68	-0.74	0.99	-0.71	1.67	-0.43	1.40	-0.50	1.25	-0.41	1.05	-0.43
SCV	0.37	-0.16	0.93	-0.36	1.18	-0.30	0.70	-0.44	1.25	-0.37	1.23	-0.42	0.90	-0.34	0.73	-0.35

4 Discussions and Conclusions

In this study, a whole heart model based on a realistic human with detailed conduction system and fiber orientation has been used to investigate the effects of conduction delay caused by LAFB and slow conduction velocity in the impaired myocardium on the activation sequence maps and 12-lead ECG. The two simulated situations showed typical characteristics of ECG criteria required for LAFB diagnosis on limb leads and chest leads. Although there were a few small differences between the two effects from the two clinical situations, their simulation results demonstrated some common ECG pattern characteristics, indicating that the LAFB induced ECG patterns can be caused either by conduction block in the left anterior fascicle or by slow conduction in the impaired myocardium. The main differences were the duration of QRS and wave amplitude. The presences of decreased amplitude and prolonged duration of QRS are good clinical indicators of impaired conduction in ventricular myocardium.

Although current interpretation of bundle branch block patterns considers the possibility that the impaired conduction may be caused by the lesion of myocardium, current diagnosis mainly focused on the conduction system. Since the impaired conduction in the myocardium may cause the similar LAFB ECG patterns, our simulations provided a promising starting point for investigating LAFB in heart failure patients, which would provide some references for clinical diagnosis.

It should be pointed out that there are several limitations in the present study. In our simulation only the impaired myocardium located at the left ventricle anterior wall was considered, the effects of impaired myocardium from other locations and the extent of areas have not been simulated. Secondly, the parameters of cell model have not been comprehensively investigated, only the conduction velocity was changed without considering the ion channel mechanisms. Finally the model used in this study was a static heart model with electrophysiological properties, but the mechanical functions have not been considered. Cardiac motion should be considered in future studies to further improve the simulation accuracy.

Acknowledgements

This project is supported in part by the National Natural Science Foundation of China (61527811).

References

[1] M. V. Elizari, R. S. Acunzo and M. Ferreiro, "Hemiblocks Revisited," *Circulation*, Vol. 115, no. 9, pp. 1154-1163, 2007.

[2] M. C. Mandyam, E. Z. Soliman, S. R. Heckbert, E. Vittinghoff and G. M. Marcus, "Long-term outcomes of left anterior fascicular block in the absence of overt cardiovascular disease," *Jama the Journal of the American Medical Association*, Vol. 309, no. 15, pp. 1587-1588, 2013.

[3] J. B. Nielsen, S. E. Strandberg, A. Pietersen, C. Graff, A. G. Holst and C. E. Study, "Left anterior fascicular block and the risk of cardiovascular outcomes," *Jama Internal Medicine*, Vol. 174, no. 6, pp. 1001-1003, 2014.

[4] R. S. Acunzo, I. V. Konopka, R. A. Sanchéz, N. Pizzarelli, F. C. Wells, A. Baranchuk and P. A. Chiale, "Right bundle branch block and middle septal fiber block with or without left anterior fascicular block manifested as aberrant conduction in apparent healthy individuals: Electro-vectorcardiographic characterization," *Journal of Electrocardiology*, Vol. 46, no. 2, pp. 167-172, 2013.

[5] Q. Lu, X. Lu and X. Tan, "The clinic significance and prognosis of IRBBB+LAFB and LAFB in organic heart disease," *Chinese Journal of Health Care & Medicine*, Vol., no. pp. 2015.

[6] K. T. Nguyen, E. Vittinghoff, T. A. Dewland, M. C. Mandyam, P. K. Stein, E. Z. Soliman, S. R. Heckbert and G. M. Marcus, "Electrocardiographic Predictors of Incident Atrial Fibrillation," *American Journal of Cardiology*, Vol. 118, no. 5, pp. 714-719, 2016.

[7] A. Auricchio, C. Fantoni, F. Regoli, C. Carbucicchio, A. Goette, C. Geller, M. Kloss and H. Klein, "Characterization of left ventricular activation in patients with heart failure and left bundle-branch block," *Circulation*, Vol. 109, no. 9, pp. 1133-1139, 2004.

[8] D. Prochnau, H. Kuehnert, M. Heinke, H. R. Figulla and R. Surber, "Left Ventricular Lead Position and Nonspecific Conduction Delay Are Predictors of Mortality in Patients During Cardiac Resynchronization Therapy," *Canadian Journal of Cardiology*, Vol. 27, no. 3, pp. 363–368, 2011.

[9] R. Eschalier, S. Ploux, P. Ritter, M. Haïssaguerre, K. A. Ellenbogen and P. Bordachar, "Nonspecific intraventricular conduction delay: Definitions, prognosis, and implications for cardiac resynchronization therapy," *Heart Rhythm the Official Journal of the Heart Rhythm Society*, Vol. 12, no. 5, pp. 1071-1079, 2015.

[10] F. G. Akar, D. D. Spragg, R. S. Tunin, D. A. Kass and G. F. Tomaselli, "Mechanisms Underlying Conduction Slowing and Arrhythmogenesis in Nonischemic Dilated Cardiomyopathy," *Circulation Research*, Vol. 95, no. 7, pp. 717-725, 2004.

[11] J. A. Milliken, "Isolated and complicated left anterior fascicular block: A review of suggested electrocardiographic criteria," *Journal of Electrocardiology*, Vol. 16, no. 2, pp. 199-211, 1983.

[12] L. Bacharova, V. Szathmary and A. Mateasik, "Electrocardiographic patterns of left bundle-branch block caused by intraventricular conduction impairment in working myocardium: a model study," *Journal of Electrocardiology*, Vol. 44, no. 6, pp. 768-778, 2011.

[13] N. Varma, P. Jia and Y. Rudy, "Electrocardiographic imaging of patients with heart failure with left bundle branch block and response to cardiac resynchronization therapy," *Journal of Electrocardiology*, Vol. 40, no. 6 Suppl, pp. S174–S178, 2007.

[14] D. Deng, P. Jiao, X. Ye and X. Ling, "An Image-Based Model of the Whole Human Heart with Detailed Anatomical Structure and Fiber Orientation," *Computational & Mathematical Methods in*

Medicine, Vol. 2012, no. 3, pp. 449-461, 2012.

[15] D. D. Deng, Y. L. Gong, G. F. Shou, P. F. Jiao, H. G. Zhang, X. S. Ye and L. Xia, "Simulation of biatrial conduction via different pathways during sinus rhythm with a detailed human atrial model," *Journal of Zhejiang Universityence B*, Vol. 13, no. 9, pp. 676-694, 2012.

[16] M. Courtemanche, R. J. Ramirez and S. Nattel, "Ionic mechanisms underlying human atrial action potential properties: insights from a mathematical model," *American Journal of Physiology*, Vol. 275, no. 2, pp. 301-321, 1998.

[17] K. H. W. J. T. Tusscher, N. D., N. P. J. and P. A. V., "A model for human ventricular tissue," *American Journal of Physiology Heart & Circulatory Physiology*, Vol. 286, no. 4, pp. H1573-H1589, 2004.

[18] Y. Zhang, L. Xia, Y. Gong, L. Chen, G. Hou and M. Tang. "Parallel Solution in Simulation of Cardiac Excitation Anisotropic Propagation," *Functional Imaging and Modeling of the Heart, International Conference*, Vol. 4466, pp. 170-179, 2007.

[19] D. Durrer, R. T. V. Dam, G. E. Freud, M. J. Janse, F. L. Meijler and R. C. Arzbaecher, "Total excitation of the isolated human heart," *Circulation*, Vol. 41, no. 6, pp. 899-912, 1970.